J. Membrane Biol. 206, 43–51 (2005)
DOI: 10.1007/s00232-005-0772-5

The Journal of
Membrane
Biology

Aldosterone Reduces Crypt Colon Permeability during Low-Sodium Adaptation

M. Moretó[1], E. Cristià[1], A. Pérez-Bosque[1], I. Afzal-Ahmed[2], C. Amat[1], R.J. Naftalin[2]
[1]Departament de Fisiologia, Facultat de Farmàcia, Universitat de Barcelona, Barcelona, Spain
[2]Physiology Division, King's College London, Guys Campus, London, UK

Received: 26 August 2005

Abstract. Fluid and electrolyte absorption by colonic crypts depends on the transport properties of crypt cellular and paracellular routes and of the pericryptal sheath. As a low-Na^+ diet increases aldosterone and angiotensin II secretion, either hormone could affect absorption. Control and adrenalectomized (ADX) Sprague-Dawley rats were kept at a high-NaCl (HS) diet and then switched to low-NaCl (LS) diet for 3 days. Aldosterone or angiotensin II plasma concentrations were maintained using implanted osmotic mini-pumps. The extracellular Na^+ concentration in isolated rat distal colonic mucosa was determined by confocal microscopy using a low-affinity Na^+-sensitive fluorescent dye (Sodium red, and Na^+-insensitive BODIPY) bound to polystyrene beads. Crypt permeability to FITC-labelled dextran (10 kDa) was monitored by its rate of escape from the crypt lumen into the pericryptal space. Mucosal ion permeability was estimated by transepithelial electrical resistance (TER) and amiloride-sensitive short-circuit current (SCC). The epithelial Na^+ channel, ENaC, was determined by immunolocalization. LS diet decreased crypt wall permeability to dextran by 10-fold and doubled TER. Following ADX, aldosterone decreased crypt wall dextran permeability, increased TER, increased Na^+ accumulation in the pericryptal sheath and ENaC expression even in HS. Infusion of angiotensin II to ADX rats did not reverse the effects of aldosterone deprivation. These findings indicate that aldosterone alone is responsible for both the increase in Na^+ absorption and the decreased paracellular and pericryptal sheath permeability.

Key words: Aldosterone — Angiotensin II — Colon — Permeability

Correspondence to: M.Moretó; email: mmoreto@ub.edu

Introduction

The major function of rat and human distal colon is absorption of NaCl and water. Aldosterone is thought to be the key hormone in the regulation of Na^+ homeostasis, however, colonic absorptive function depends not only on active Na^+ transport across crypt luminal cells, but also on the myofibroblast cells of the surrounding pericryptal sheath. This matrix generates a barrier to macromolecules and NaCl diffusion, thereby promoting and maintaining NaCl accumulation within the space lying between the colonocytes and the sheath. This hypertonic "central" compartment generates an osmotic gradient across the cells between the crypt lumen and pericryptal space and a hydrostatic pressure gradient across the sheath, which forces fluid outflow into the interstitial space outside the sheath (Naftalin & Pedley, 1999).

Colonic Na^+ absorption is influenced by a low-sodium diet. Low NaCl concentrations at the macula densa segment of the renal distal tubule increase renin secretion into the blood, thereby activating the renin-angiotensin-aldosterone system (RAAS). Renin cleaves angiotensinogen secreted by the liver to angiotensin I. Angiotensin I is then cleaved by angiotensin-converting enzyme (ACE) to angiotensin II (ANG II). Thereafter, ANG II increases aldosterone (ALDO) secretion by stimulating its synthesis in the adrenal zona glomerulosa (Peart, 1969). In addition to this classical pathway of ANG II synthesis, tissue RAAS have been identified in a number of organs, suggesting that various tissues have the ability to synthesize ANG II independently of the circulating RAAS (Paul, Wagner & Dzar, 1993). Tissue-specific RAAS may be present in the kidney, brain, vasculature, adrenal, heart (Campbell & Habener, 1986) and colon (Hirasawa et al., 2002).

In rat hearts exposed to raised concentrations of ANG II and ALDO, there is proliferation of myofibroblasts and an increase of collagen (Campbell,

Janieki & Weber, 1995). So, apparently, both angiotensin II and aldosterone have roles in inducing cardiac fibrosis. Colonic mucosal fibrosis is induced as a chronic reaction to radiation and can be reversed by long-term treatment with the ACE inhibitor captopril (Thiagarajah et al., 2002). Fibrosis in lung, kidney, heart and brain following radiation or as a consequence of chronic inflammation have also been described and are ameliorated by ACE inhibitors or angiotensin antagonists like losartan (Molteni, Moulder & Cohen, 2000; Naftalin, 2004).

As colonic absorptive function depends on crypt luminal cells and on myofibroblasts and as Na^+ depletion upregulates both ALDO and ANG II secretion, it is important to delineate the role of each hormone in each component of colonic permeability. The aim here is to investigate the separate roles of aldosterone and angiotensin II in the structural and functional adaptations of the colon in response to changes in dietary Na^+ intake.

Materials and Methods

Experimental Animals

Studies were performed on adult male Sprague-Dawley rats (Harlan Iberica, Barcelona, Spain) weighing 200–250 g the day of experiment. They were housed one per cage under 12:12 h light-dark cycle and food and water were available *ad libitum*. Experimental procedures were approved by the Ethical Committee for Animal Experimentation of the Universitat de Barcelona.

Experimental Protocols

Protocol 1: Experimental Protocol for Examining Effect of Diets and Pharmacological Treatment

Animals received a high-sodium diet (HS, wheat and barley plus 150 mM NaCl in drinking water). After 4 days the diet of some animals was altered to a low-sodium diet (LS, wheat and barley and drinking water containing 150 μM NaCl) for 3 days. In preliminary studies the rats were fed a LS diet for 1, 3, 5 and 7 days. These results showed that there were significant effects after 3 days, so the subsequent experiments were done only using the 3-day time period. Groups of rats received the angiotensin converting enzyme (ACE) inhibitor, captopril (CAP) or the angiotensin II receptor type I (AT1) inhibitor, losartan (LOS), or the aldosterone antagonist, spironolactone (SPI). Captopril and losartan were administered in drinking water at a dose of 65 mg/kg·day and 30 mg/kg·day, respectively, and spironolactone (10 mg/kg·day) was given by gavage, suspended in water containing 25% propylene glycol.

Protocol 2: Experimental Protocol of ADX Followed by Hormonal Replacement

Some rats were anesthetized with isofluorane (Inibsa®, Spain) and were adrenalectomized (ADX) via bilateral flank incisions. At the time of ADX, osmotic minipumps (model 2002, Alzet, Palo Alto, CA) were implanted subcutaneously in the neck of each rat. Two hormones were replaced using minipumps: D-aldosterone (Sigma) dissolved in propylene glycol, was delivered at a rate of 450 μg/kg day (ALDO groups) and angiotensin II (Sigma) dissolved in saline, was delivered at a rate of 288 μg/kg day (ANG II groups). Groups without hormonal replacement were implanted with pumps delivering vehicle alone. The pumps were equilibrated with saline overnight before insertion. Both ALDO and ANG II plasma concentrations are chronically increased with this protocol.

All ADX groups received dexamethasone with the osmotic minipumps. Dexamethasone was chosen as a representative glucocorticoid because it binds more selectively to the glucocorticoid receptor than corticosterone, the predominant endogenous glucocorticoid in the rat (Funder et al., 1973). A dexamethasone dose of 12 μg/kg day was chosen as the lowest dose necessary for maintenance of normal weight gain, glomerular filtration rate and normal fasting plasma glucose and insulin levels (Stanton et al., 1985).

After surgery the animals were kept on the HS diet during 4 days. Thereafter, half of the animals were changed to LS diet for 3 days and the other half continued with HS diet. With this protocol we obtain 6 groups with different hormonal profile: ADX·HS + ALDO, ADX·HS + ANG, ADX·HS, ADX·LS + ALDO, ADX·LS + ANG, and ADX·LS.

Tissue Preparation

Rats from both protocols were maintained in metabolic cages during the last three days, and 24-h urinary output, water intake, food consumption and weight increase were measured daily. Urinary volume, osmolality, Na^+ and K^+ concentrations, ANG II and ALDO concentrations were also measured. To prevent urinary bacterial growth, azlocillin (0.5 mg, Sigma) was added to the collection tube. Thereafter, rats were anaesthetized with ketamine/xylacine (100/10 mg/kg) i.p.; the descending colon was removed rapidly and the contents were removed by washing with PBS. Colonic mucosa was isolated from the muscularis mucosae by scraping with a glass slide and maintained in Earl's medium for its use in in vitro functional studies (pericryptal Na^+ concentration, dextran permeability), or fixed in 4% paraformaldehyde in PBS at 4°C for 24 h for immunohistochemistry studies. The tissue was washed and stored in PBS at 4°C. Trunk blood was collected in tubes containing EDTA (1.5 mg/ml of blood) and a protease inhibitor cocktail (Sigma) and kept on ice until centrifugation at 4°C. Plasma was aliquoted and stored at −80°C for subsequent assay of plasma hormone and ion concentrations.

Plasma and Urinary Ion Concentration

Plasma K^+ and Na^+ concentrations were measured using potentiometric direct dry chemistry (Beckman Coulter Corporation). Their urinary concentrations were determined using inductively coupled plasma optical emission spectroscopy (ICP-OES Thermo Jarrell Ash model ICAP 61E, Genesis Laboratories Systems Inc., Colorado).

Hormone Determinations

Urine and plasma hormones were determined by RIA using commercially available kits: ALDOCTK-2, DiaSorin S.p.A. (Italy) for urinary aldosterone, Aldosterone RIA kit Immunotech for plasma aldosterone and RIA I^{125} Bühlmann Laboratories (Switzerland) for plasma angiotensin II.

Electrical Parameters

Freshly excised segments of distal colon were mounted in the Ussing chambers. The volume of the bathing solution in each chamber was 4 ml with a tissue internal surface area of 0.63 cm^2. The Krebs

bathing solution buffer contained (in mM) 115 NaCl, 25 $NaHCO_3$, 2 KH_2PO_4, 8 KCl, 1.2 $CaCl_2$, 1.1 $MgCl_2 \cdot 6H_2O$. Glucose (10 mM) was added to the buffer bathing the serosal side of the tissue, and this was osmotically balanced by addition of 10 mM mannitol to the mucosal buffer. Each solution was continuously oxygenated with 95% O_2-5% CO_2 and circulated by gas lift, pH 7.4 and 37°C. Two pairs of Ag/AgCl electrodes monitored the transmural potential difference (*PD*, mV) under open-circuit conditions or the short-circuit current (I_{sc}, $\mu A/cm^2$) with transmural *PD* clamped to zero using voltage clamp (Dipl.-Ing. K. Mussler Scientific Instruments, Aachen, Germany) connected to a PC equipped with clamp-specific software (Clamp v.2·14, Aachen, Germany). Transepithelial electrical resistance (*TER*; $ohm \cdot cm^2$) was obtained from the clamp program by constant current pulses at 15 s intervals. Experiments were carried out simultaneously in six chambers. After a 30-min equilibration period, *PD*, I_{sc} and *TER* were recorded in the basal state every 6 s under voltage-clamp conditions and after addition of apical amiloride (0.1 mM) to measure basolateral Na^+ pump activity, over a period of 1 h in Krebs.

Pericryptal Na^+ Accumulation

Na^+ concentration in isolated rat distal colonic mucosa was determined using a modification of a dual-wavelength laser scanning confocal microscopic method in which low affinity Na^+-sensitive dye (Sodium Red, and BODIPY-fl) are bound to microscopic polystyrene beads (Jayaraman et al., 2001). Fifty mg of sodium red (sample provided by Molecular Probes, Eugene, OR; catalog no. 71351) and 30 μg of BODIPY-fl in 2% methanol-water were added to a 1% (vol/vol) suspension of 50-nm-diameter carboxyl latex beads (Polymer Lab, Amherst, MA) suspended in 4 ml of water. The chromophores remained quantitatively immobilized on the beads during measurements and for > 2 months of storage in water at 4°C in the dark. Colonic mucosal pieces were loaded with the dye-containing beads with 200 μl of a 10% (vol/vol) solution by incubation for 1 h. The method used here uses smaller beads than previously (Thiagarajah et al., 2001a). This improves the rate of bead uptake into the extracellular space and makes better contrast and delineation of the extracellular Na^+ concentration. The local Na^+ concentration was estimated by ratiometric imaging of the beads using the Na^+ red signal, which increases linearly in the concentration range 0–500 mM and the green signal from BODIPY-fl.

Na^+ Ratio Analysis

Image pairs of sodium red and BODIPY-fl were acquired from the same field. Background images were obtained under the same conditions but without loading with the dye. Analysis was performed using Image J software http://rsb.info.nih.gov. Ratio images (red-to-green fluorescence) were obtained by pixel-by-pixel division of background-subtracted images. Background values were < 10% of signal. Averaged ratios were obtained by integration of red and green fluorescence intensities over specified regions of interest. Two to three crypts were measured from each set of images.

Dextran Permeability

Crypt permeability to dextran was monitored by the rate of escape of fluorescein isothiocyanate (FITC)-labeled dextran (molecular weight 10,000, FITC dextran; Sigma Chemicals, St Louis, MI) from the crypt lumen into the pericryptal space at 37°C. Crypt luminal and pericryptal concentration of FITC-dextran were estimated by monitoring the ratio of fluorescence intensity of each zone. The procedures performed were as described (Naftalin, Zammit & Pedley, 1999).

Immunocytochemistry

Colonic mucosal tissue (0.5 cm^2 pieces) was placed in 1.5 ml Eppendorf tubes and were permeabilized in 0.2% Triton X-100 in blocking buffer (1% BSA in PBS and glycine) for 30 min. Samples were washed three times in PBS and incubated for 90 min with rabbit anti-rat γ-ENaC antibody (1:100, Alpha Diagnostics Intl., San Antonio, TX), washed 3 × in PBS and then incubated for 60 min in secondary anti-rabbit Alexa-488 antibody (Molecular Probes, Eugene, OR) diluted 1:100 with PBS and washed again 3 × in PBS.

Confocal Images

Each piece of tissue was viewed from the mucosal side with the confocal microscope using a 20× or 40× Leica SPII oil immersion lens. The focus plane was taken to the surface of the tissue and images were captured at 2.5 μm or 5 μm steps using the automatic Z-step motor. Images were taken from 0 μm down to 40 μm below the surface. With dextran permeability measurements, the scans were repeated at 5 min intervals for 20 min. For Na^+-red ratio imaging, the tissues were pre-incubated at 37°C in a humidified hood for 30 min with the dye prior to viewing with the confocal microscope. This allows the dye beads to penetrate into the pericryptal and interstitial spaces. The captured images represent the general level of staining throughout the whole tissue and were obtained with the same optical conditions, gain and section size.

Image Analysis

The captured images were analyzed using the program Image J (Image J 1.32, http://rsb.info.nih.gov/ij/index.html) (Rasband, 1997–2005) to quantify the fluorescence from each antibody (Abramoff, Magelhaes & Ram, 2004). The fluorescence was quantified by areas, which were divided into either crypt or inter-crypt and were taken by selecting a region of interest within the relevant part of the image. Three areas of both crypt and inter-crypt regions were taken for image analyses and therefore there were thirty measurements per tissue at the various depths. The mean and SEM of the measurements after background subtraction from each image were calculated. To obtain averaged fluorescence intensities within the crypt lumen and pericryptal sheath, projected images using maximal intensity averaging over the depths 5–30 μm were obtained for each rat and results compared for each condition.

Statistical Analyses

Data were expressed as means ± SEM. Comparisons between HS and LS diet were made by ANOVA using SPSS-10.0 software (SPSS). To analyze the effects of pharmacological treatment, groups were compared with the LS group by ANOVA followed by Scheffe's *post-hoc* test. In ADX groups, the groups with ALDO or ANG II replacement were compared with the groups without supplementation by ANOVA followed by Scheffe's *post-hoc* test. In results of electrical parameters, the effect of amiloride was tested by ANOVA. Differences were considered statistically significant when the test yielded $P < 0.05$.

Results

Metabolic and Hormonal Changes

The physiological variables relating to body weight, food and water intake, and to urinary function,

Table 1. Functional data from rats in protocol 1

Protocol 1	Units	HS	LS 3D	LS 3D CAP	LS 3D LOS	LS 3D SPI
Weight gain (3 days)	g	7.9 ± 1.1 (7)	6.3 ± 0.6 (7)	−2 ± 1.0 (6)$^{\#}$	−0.8 ± 0.7 (5)$^{\#}$	−0.1 ± 1.6 (5)$^{\#}$
Food consumption (3 days)	g	63 ± 3.1 (8)	63 ± 3.8 (8)	53 ± 3.7 (5)$^{\#}$	52 ± 3.6 (5)*	57 ± 3.9 (5)$^{\#}$
Water intake (3 days)	ml	84 ± 6.3 (8)	68 ± 4.8 (8)	73.3 ± 6.7 (5)	127 ± 16.1 (5)$^{\#}$	138 ± 22.2 (5)$^{\#}$
Urine volume (3 days)	ml	35.3 ± 3.7 (8)	30.47 ± 4.2 (8)	42.2 ± 2.1 (5)$^{\#}$	99.7 ± 19.4 (5)$^{\#}$	110.7 ± 17.9 (5)$^{\#}$
Urinary Na^+ (3 days)	mmol	8.87 ± 0.73 (6)	0.28 ± 0.06 (7)*	0.13 ± 0.01 (4)*	0.09 ± 0.02 (4)*	0.11 ± 0.03 (4)*
Urinary K^+ (3 days)	mmol	4.28 ± 0.28 (6)	4.09 ± 0.18 (7)	3.9 ± 0.96 (4)	3.96 ± 0.51 (4)	4.41 ± 0.33 (4)
Na^+ plasma at day 3	mM	142.1 ± 1.2 (6)	143.9 ± 1.1 (6)	141.7 ± 0.7 (6)	143.7 ± 1.7 (7)	145.6 ± 0.5 (7)
K^+ plasma at day 3	mM	4.48 ± 0.31 (6)	4.23 ± 0.15 (6)	4.62 ± 0.26 (6)	4.45 ± 0.22 (7)	4.36 ± 0.14 (7)
Cl^- plasma at day 3	mM	100.1 ± 0.9 (6)	100.6 ± 0.5 (6)	98.1 ± 0.7 (6)	101.3 ± 1.5 (7)	101.9 ± 0.3 (7)
Aldosterone plasma	nM	0.63 ± 0.07 (4)	1.21 ± 0.27 (7)*	0.60 ± 0.17 (5)$^{\#}$	0.73 ± 0.12 (5)*	2.98 ± 0.71 (5)$^{\#}$
Angiotensin II plasma	pg/ml	57.8 ± 4.8 (5)	85.8 ± 9.9 (7)*	60.05 ± 3.9 (5)*	95.7 ± 8.9 (5)	141.5 ± 23.5 (5)$^{\#}$

Protocol 1 involves rats fed HS or LS diets and rats treated with captopril (CAP), losartan (LOS) and spironolactone (SPI). Variables with the expression "3 days" include the results obtained by summing the results of the three last days before sacrifice; the expression "at day 3" refers to variables measured during the third day in the metabolic cage. Values are means ± SEM (in parentheses, the number of animals). *$P < 0.001$ HS *vs.* LS; $^{\#}P < 0.001$ LS *vs.* pharmacological treatment.

plasma ion and hormone concentrations are shown in Tables 1 (protocol 1) and 2 (protocol 2).

Plasma concentrations of aldosterone and angiotensin II are significantly increased after 3 days in the LS diet, compared with the HS diet (Table 1). Of the six groups obtained following adrenalectomy (ADX) the two with ALDO replacement (protocol 2) have high plasma concentrations of aldosterone and the other four, very low levels, as expected (Table 2). It is worth noting that the ADX·LS + ALDO group has a low ANG II plasma concentration, suggesting that high circulating aldosterone concentrations may inhibit RAAS directly or indirectly. ANG II infusion raised the circulating concentration of this hormone in ADX·HS + ANG and ADX·LS + ANG groups (Table 2). Urinary aldosterone excretion in 3 days following dietary switch from HS to LS is raised from 51 ± 5.6 pmol to 201 ± 51.4 pmol ($n = 6$) but is negligible in the 3 days post ADX. The polydipsia and polyuria as well as K^+ depletion observed in the ADX·HS + ALDO are consistent with characteristics of the Conn's syndrome (Fardella & Mosso, 2002).

The key physiological variables relating to aldosterone function are that net Na^+ loss during 3 days with LS diet following ADX is raised without ALDO supplementation; with ALDO replacement, urinary Na^+ loss is half that seen without ALDO replacement, or with ANG II replacement (Table 2). Weight loss correlates with these findings. With an LS diet following ADX, in animals without ALDO supplement, there is net weight loss; whereas ALDO supplementation prevents weight loss. ANG II supplementation without ALDO increases weight loss (Table 2).

Another indicator of low aldosterone activity following ADX is the high plasma K^+ concentration seen without ALDO supplementation (Table 2). This shows that K^+ excretion via the urine and faeces fails to match the rise in plasma K^+ concentration. These findings indicate that the dietary, surgical and pharmacological treatments were efficacious.

Effect of HS and LS Diet and Aldo Supplementation post ADX on Rat Distal Colon Electrical Parameters

Table 3 shows that in LS conditions there are significant increases in PD, I_{sc} and *TER* compared with HS conditions ($P < 0.01$). Amiloride (0.1 mM) abolishes the *PD* and I_{sc} but does not affect the LS-dependent increase in *TER*. In ADX rats following ALDO replacement in both HS and LS there are similar increases in *PD*, I_{sc} and electrical resistance. The LS and aldosterone-dependent increases in I_{sc} and *PD* abolished by amiloride (0.1 mM) are similar to those found by many others (Fromm & Hegel, 1978; Horster et al., 1994). However the increase in *TER* is only observed by a few, some observe a decrease, whilst others find no change in *TER* (Dolman, Edmonds & Salas-Coll 1978; Schulzke, Fromm & Hegel, 1986). The large increase in *TER* observed here may relate to the time of exposure to the hormone *in vivo* prior to measurement in vitro. The concurrent effects of dextran permeability develop over 3–5 days. Much smaller effects are observed after 24 hours.

Effect of HS and LS Diet and ALDO or ANG II Supplementation post ADX on Rat Distal Colon Permeability to Dextran

The crypt wall permeability to dextran determined from the rate of escape of FITC-labeled dextran (10 kDa) from the crypt lumen into the pericryptal space was used as an index of the permeability of the pericryptal barrier (Thiagarajah et al., 2001b). During the

Table 2. Functional data from rats in protocol 2

Protocol 2	Units	ADX HS+ALDO	ADX HS+ANG	ADX HS	ADX LS+ALDO	ADX LS+ANG	ADX LS
Weight gain (3 days)	g	3.6 ± 1.7 (8)	7.5 ± 3.1 (7)	2.5 ± 2.2 (8)	4.9 ± 1.7 (8)	−29.6 ± 5.7 (8)*	−12.8 ± 2.7 (8)*
Food consumption (3 days)	g	64 ± 1.2 (8)	57 ± 5.5 (7)	54 ± 1.7 (8)	63 ± 1.0 (8)	19 ± 4.4 (8)*	38 ± 0.3 (8)*
Water intake (3 days)	ml	184 ± 28.6 (8)*	82 ± 5.5 (7)	91 ± 6.8 (8)	61 ± 5.1 (8)	23 ± 5.7 (8)	50 ± 4.2 (8)
Urine Volume (3 days)	ml	125.6 ± 28.2 (8)*	38.9 ± 3.9 (7)	49.2 ± 6.9 (8)	23.7 ± 4.1 (8)	17.1 ± 2.8 (8)	32.4 ± 1.1 (8)
Urinary Na^+ (3 days)	mmol	24.18 ± 4.21 (8)	8.76 ± 0.69 (7)	10.55 ± 1.19 (8)	0.83 ± 0.04 (7)	1.82 ± 0.36 (6)	1.63 ± 0.15 (8)
Urinary K^+ (3 days)	mmol	3.69 ± 0.38 (8)	3.4 ± 0.24 (7)	3.47 ± 0.13 (8)	2.02 ± 0.32 (8)	1.98 ± 0.14 (6)	3.06 ± 0.13 (8)
Urine osmolality at day 3	mosm/kg	626 ± 51.7 (8)	1081 ± 78.4 (7)	1142 ± 108.1 (8)	1233 ± 221.6 (8)	1055 ± 285.2 (8)	699 ± 54.1 (8)
Urine mosm (3 days)	mosm	71.13 ± 9.11 (8)	39.08 ± 2.17 (7)	41.77 ± 2.93 (8)	22.09 ± 0.97 (8)	16.36 ± 0.96 (6)	21.16 ± 0.63 (8)
Na^+ plasma at day 3	mM	134.8 ± 1.0 (5)	140.9 ± 2.5 (8)	127.5 ± 1.4 (5)	141.3 ± 4.6 (6)	138.2 ± 1.9 (8)	131.5 ± 2.4 (5)
K^+ plasma at day 3	mM	2.95 ± 0.26 (5)*	5.95 ± 0.28 (8)	5.34 ± 0.21 (5)	4.93 ± 0.37 (6)	7.27 ± 0.50 (8)*	7.38 ± 0.37 (5)*
Cl^- plasma at day 3	mM	90.3 ± 1.7 (5)	92.5 ± 2.7 (8)	93.3 ± 1.7 (5)	99.7 ± 4.6 (6)	81.9 ± 1.5 (8)	87.46 ± 3.9 (5)
Aldosterone plasma	nM	13.6 ± 4.8 (6)*	0.015 ± 0.008 (5)	0.006 ± 0.001 (7)	12.4 ± 1.5 (6)*	0.006 ± 0.001 (7)	0.020 ± 0.006 (6)
Angiotensin II plasma	pg/ml	55 ± 5.6 (5)	104 ± 23 (5)*	65 ± 5 (5)	56 ± 7.5 (5)	116 ± 17.2 (5)*	125.7 ± 17.8 (8)*

Protocol 2 involves adrenalectomized rats with hormonal replacement. Variables with the expression "3 days" include the results obtained by summing the results of the three last days before sacrifice; the expression "at day 3" refers to variables measured during the third day in the metabolic cage. Values are means ± SEM (in parentheses, the number of animals). *$P < 0.05$.

transition from an HS diet to an LS diet, there is an ≈ 10-fold decrease in crypt dextran permeability (Fig. 1*C* and Table 4). This decrease in permeability is prevented by pharmacological treatments which either prevent aldosterone synthesis (captopril or losartan) or inhibit the effect of aldosterone on the mineralocorticoid receptor (spironolactone) (Table 4). Following ADX, no decrease in dextran permeability is observed with LS diet (Table 5). However, when ADX rats, in both LS and HS conditions, are perfused with ALDO, crypt permeability to dextran is decreased ($P < 0.01$). Results from ADX rats perfused with ANG II, also show that ANG II on its own does not induce any decrease in crypt wall permeability to dextran. On the contrary, in both HS and LS conditions, the permeability to dextran increases ($P < 0.05$).

Effect of HS and LS Diet and ALDO or ANG II Supplementation post ADX on Pericryptal Na^+

Within three days of changing from HS to LS diet there is an effect on Na^+ transport in rat distal colon, evident from the raised sodium accumulation in the pericryptal spaces (Table 4). Na^+ accumulates to a higher concentration in the pericryptal sheaths of rats with a low Na^+ intake (315 ± 20 mM; $n = 5$) than in those with high Na^+ intake (150 ± 10 mM; $n = 4$). Treatment with captopril, losartan, or spironolactone prevents the increase of Na^+ transport induced by LS diet and the increase of Na^+ accumulation in the pericryptal sheath. Projection images in the Z-plane obtained using ImageJ software show that the region of high pericryptal Na^+ starts at the crypt opening and rapidly diminishes towards isotonicity at depths below 40 μm (Figure 1*A*). This correlates with the decrease in crypt luminal [Na^+] with depth. Below a crypt luminal depth of 40–50 μm, as a result of absorption from the proximal parts of the crypt, the luminal fluid is Na^+ depleted. This retards further Na^+ absorption via the colonocytes to the pericryptal sheath. With HS diet, the pericryptal Na^+ is nearly isotonic over the entire length of the crypt and no substantial decrease in luminal [Na^+] occurs. These findings with rat colon in vitro are similar to those reported previously with mouse colon in vivo (Thiagarajah et al., 2001a).

In ADX rats, in both HS and LS conditions, ALDO perfusion results in Na^+ accumulation within the pericryptal space to ≈ 330 mM. In this condition, no significant difference is observed between the pericryptal Na^+ accumulated between HS and LS conditions. When ANG II is perfused, there is no increase in pericryptal Na^+ accumulation above that in ADX rats without any supplement (Table 5).

Table 3. Electrical parameters

	PD (mV)		I_{sc} ($\mu A/cm^2$)		*TER* (Ohm • cm^2)
	basal	+amil	basal	+amil	basal
HS	1.23 ± 0.35 (4)	0.80 ± 0.15 (4)	22.2 ± 7.7 (4)	16.0 ± 7.1 (4)	52.2 ± 3.9 (3)
LS 3D	4.04 ± 2.10 (6)*	1.85 ± 0.5 (6)†	65.6 ± 10.1 (4)*	12.2 ± 5.1 (4)†	73.9 ± 4.5 (5)*
ADX HS+ALDO	4.93 ± 1.84 (4)*	0.87 ± 0.24 (4)†	98.3 ± 18.5 (5)*	13.6 ± 4.7 (4)†	62.2 ± 1.2 (7)*
ADX HS	1.65 ± 0.20 (3)	1.56 ± 0.26 (3)	38.1 ± 10.3 (3)	42.6 ± 8.2 (3)	37.6 ± 1.3 (6)
ADX LS+ALDO	4.73 ± 0.81 (5)*	0.78 ± 0.33 (5)†	99.1 ± 26.2 (4)*	15.4 ± 7.5 (4)$^\#$	55.2 ± 3.5 (10)*
ADX LS	1.73 ± 0.82 (4)	0.89 ± 0.35 (4)	53.6 ± 21.5 (4)	38.4 ± 8.4 (4)	31.4 ± 3.1 (7)

Electrical parameters obtained in distal colon tissue from HS, rats switched to LS diet for 3 days (LS 3D), adrenalectomized rats (ADX HS, ADX LS) and supplemented with ALDO (ADX HS+ALDO, ADX LS+ALDO). Values are means ± SEM (number of animals). *$P < 0.01$ marks ALDO effect; $^\dagger P < 0.01$ marks amiloride effect.

Effect of HS and LS Diet and ALDO or ANG II Supplementation post ADX on Na^+ Transport in Rat Distal Colon

LS diet increases expression of ENaC, as shown in Table 4 (and Fig. 1*B*). The density of ENaC channel γ subunit staining with immunohistochemical methods was selected as an index of comparison between treatments, as it is strongly induced by either aldosterone or a low sodium diet (Asher et al., 1996). Treatment with captopril, losartan and spironolactone inhibits the diet-induced increase of Na^+ transport (Table 4). ENaC is often difficult to localize to the apical membranes using immunohistochemical methods (Due et al., 1994). This may be due to a large reserve present within cytosolic vesicles. What is evident here is that LS diet increases the overall expression of ENaC, as has been previously observed (Garty & Benos, 1988). In ADX rats without ALDO supplementation, there is very low ENaC expression in both HS and LS conditions, with or without ANG II supplementation (Table 5). The Table also shows that when ADX rats are perfused with ALDO, in both HS and LS conditions, ENaC expression within the colonocytes is increased ($P < 0.01$, $n = 3$).

Discussion

In this paper, functional effects of HS and LS diets and hormone replacement after ADX on distal colonic function are examined. These include Na^+ accumulation in the pericryptal space, dextran permeability across the crypt wall, the electrical variables, *PD*, I_{sc} and *TER* ± amiloride (0.1 mM) and expression of ENaC in colonocytes.

Na^+ accumulation in the pericryptal sheath in vitro depends on Na^+,K^+-ATPase activity at the crypt colonocytes' basolateral membranes, ENaC activity in the crypt colonocytes apical membranes, the rates of Na^+ leakage between the pericryptal space to the crypt lumen via the paracellular and possibly transcellular routes and from the pericryptal space across the pericryptal sheath into the interstitial space. The Na^+,K^+-ATPase activity and apical membrane ENaC expression are known to be regulated by aldosterone (Barlet-Bas et al., 1988; Asher et al., 1996). The amiloride-sensitive I_{sc} mainly reflects Na^+,K^+-ATPase activity, however, it is also a function of the ion selectivity and permeability properties of the paracellular and transcellular pathways, particularly claudin IV (Colegio et al., 2003). ENaC expression is predominantly a genomic response to aldosterone. It can also be post-translationally activated by serine proteases, e.g., prostasin (Narikiyo et al., 2002). This activation may not be entirely controlled by aldosterone (Fukushima et al., 2004). Dextran permeability between the crypt lumen and the pericryptal space is principally a function of the paracellular permeability of the crypt luminal epithelia but may also reflect the permeability of the pericryptal sheath (Thiagarajah et al., 2001a and b, 2002). Thus, by observing all the variables described here, we obtain a broad spectrum of the interrelated factors controlling the transport and permeability properties of the crypt wall. The results are in agreement with the accepted view that an LS diet leads to increased aldosterone secretion, which leads in turn to increased ENaC and Na^+,K^+-ATPase expression in the mucosal border and basolateral borders of distal colon and distal nephron and, hence, to increased Na^+ transport, demonstrated here by the aldosterone-dependent amiloride-sensitive increase in I_{sc} and *PD* and by increased Na^+ accumulation in the pericryptal sheath.

The new findings are that there is an aldosterone-sensitive decrease in crypt wall permeability to dextran which correlates with the aldosterone-dependent increase in *TER*. These changes relate to the increased Na^+ accumulation in the pericryptal space as Na^+ accumulates in part because its leakage across the crypt wall is diminished.

The effects of LS cannot be unambiguously assigned to ALDO, since LS also induces an increase in

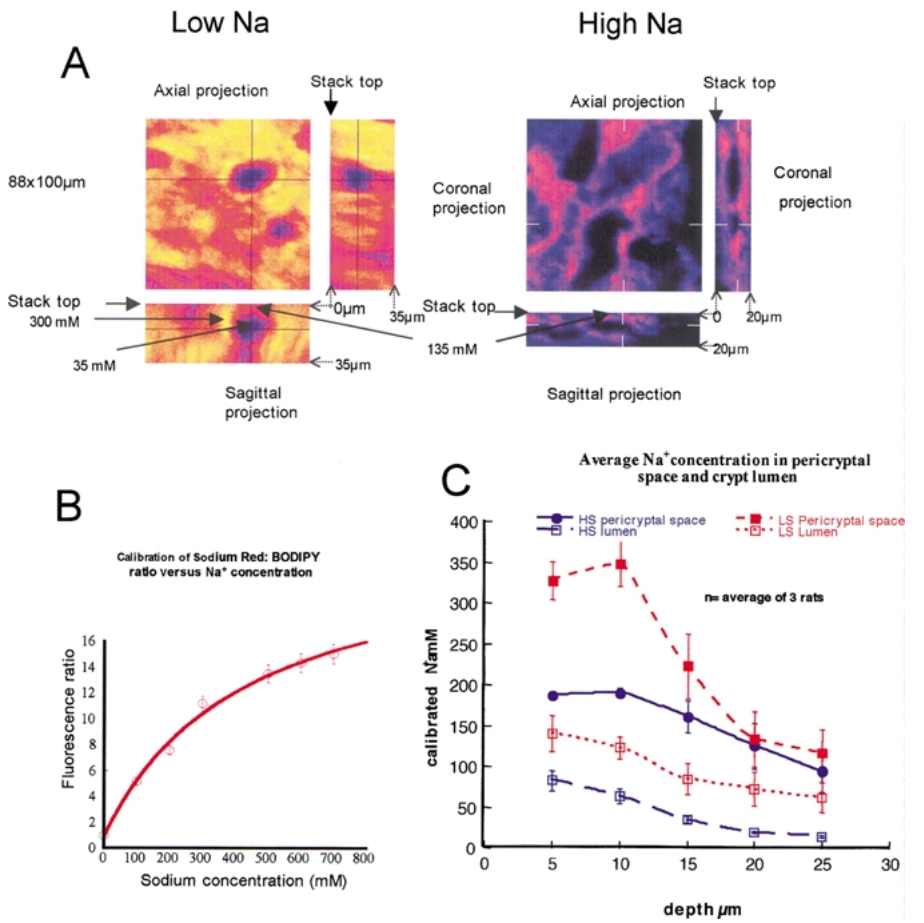

Fig. 1. Projection of stacks of confocal images of sodium red images contrasting the difference between HS and LS diet. (*A*) The projection images were obtained from stacks of ratio images taken at 0.5 μm increments in depth of colonic mucosa from HS and LS rats. These were transformed to projection images with image software (*see* Methods). The crosslines show the corresponding positions in the *x*, *y* and *z* planes in axial, coronal and sagittal sections. Thus, the sagittal projection shows the image from top at 0 μm to bottom at 35 μm depth in the stack. The color intensity varies from black to white, through red and yellow, and represents concentrations of Na^+. The Na^+ concentration in the space surrounding the crypt lumens in LS is much higher than within the lumen. The extent of these changes in Na^+ concentration with depth is shown in 1(*C*). (*B*) The pericryptal Na^+ calibrated from the ratios obtained at different Na^+ concentrations with sodium red and BODIPY-fl (*see* Methods). (*C*) The pericryptal Na^+ is on average 270–280 mM in LS rats ($n = 3$ rats) and the luminal Na^+ decreases with depth down the crypt lumen. These findings are similar to those reported by Thiagarajah et al. (2001a) for murine colon in vivo.

Table 4. Pericryptal Na^+, FITC dextran permeability and ENaC expression in Protocol 1

Protocol 1	HS	LS 3D	LS 3D CAP	LS 3D LOS	LS 3D SPI
Pericryptal Na^+ (mM)	115 ± 10 (3)	290 ± 35 (3)*	136 ± 25 (3)$^{\#}$	116 ± 12 (3)$^{\#}$	167 ± 19 (3)$^{\#}$
Dextran permeability (min^{-1})	0.023 ± 0001 (3)	0.002 ± 0.002 (3)*	0.019 ± 0.004 (3)$^{\#}$	0.029 ± 0.006 (3)$^{\#}$	0.025 ± 0.004 (3)$^{\#}$
ENaC expression (relative amount)	0.31 ± 0.05 (3)	1.01 ± 0.09 (3)*	0.38 ± 0.01 (3)*	0.14 ± 0.10 (3)$^{\#}$	0.45 ± 0.02 (3)$^{\#}$

All experiments were carried out in the distal colon segment from rats fed HS or LS diets and rats treated with captopril (CAP), losartan (LOS) and spironolactone (SPI). Values are means ± SEM. (number of animals). *$P < 0.001$ HS *vs.* LS; $^{\#}P < 0.001$ LS *vs.* pharmacological effect.

ANG II, which has been implicated in myofibroblast trophic changes in a number of tissues (Weber, 1997). For this reason, a study of the effects of ANG II and ALDO replacement following ADX in both HS and LS conditions was made to determine if dextran permeability is related to angiotensin II levels.

From the results here, it is evident that angiotensin II alone has no significant effect on Na^+

Table 5. Pericryptal Na^+, FITC dextran permeability and ENaC expression in Protocol 2

Protocol 2	ADX HS+ALDO	ADX HS+ANG	ADX HS	ADX LS+ALDO	ADX LS+ANG	ADX LS
Pericryptal Na^+ (mM)	324 ± 26 (4)*	178 ± 28 (5)	249 ± 19 (5)	331 ± 12 (4)*	172 ± 11 (5)	217 ± 13 (4)
Dextran permeability (min^{-1})	0.005 ± 0.002 (5)*	0.118 ± 0.002 (4)$^{\#}$	0.026 ± 0.004 (5)	0.005 ± 0.002 (4)*	0.054 ± 0.008 (4)$^{\#}$	0.026 ± 0.003 (4)
ENaC expression (relative amount)	0.70 ± 0.090 (3)*	0.100 ± 0.060 (4)	0.03 ± 0.1 (3)	1 ± 0.2 (3)*	0.25 ± 0.07 (4)	0.170 ± 0.090 (4)

All experiments were carried out in the distal colon segment from ADX rats and supplemented with aldosterone, angiotensin II or saline. Values are means ± SEM (number of animals). *$P < 0.01$ marks ALDO effects; $^{\#}P < 0.05$ marks Ang II effects.

transport across the crypt wall and does not reverse the HS-induced increase in crypt wall permeability to dextran. In fact, we found that dextran permeability is raised in ADX animals perfused with ANG II.

There are reports that adrenomedullin, blockade of the angiotensin II receptor I or raised intracellular cAMP can all reverse the angiotensin II-induced increases in fibrosis (Klahr & Morrissey, 1997; Swaney et al., 2005; Tsuruda et al., 2005). It is possible that ANG II without ALDO leads to breakdown of the extracellular matrix, possibly by adrenomedullin activation of matrix metalloproteinases, by as shown by Tsuruda et al. (2004). This could explain both the angiotensin II-dependent increase in dextran permeability reported here and the angiotensin II-dependent decrease in colonic transepithelial potential difference found previously (De los Rios et al., 1980).

These findings coupled with the aldosterone-dependent decrease in dextran permeability indicate that aldosterone acts not only on Na^+ transport via ENaC, Na^+, K^+-ATPase and membrane K^+ channels, but also on the less well characterized paracellular pathway. It has recently been reported that dexamethasone increases junctional proteins like claudin IV in confluent sheets of H441 lung adenocarcinoma cells prior to appearance of amiloride blockable accumulation in Na^+ domes (Shlyonsky et al., 2005). This finding is very similar to the situation observed here and reported more extensively in the companion paper (Cristià et al., 2005).

The overall conclusion is that aldosterone or mineralocorticoids, not only induce proteins which control transcellular Na^+ transport but also induce the junctional proteins which are necessary to maintain vectorial transport across epithelia and without which neither net fluid nor electrolyte flow can exist. In the descending colon, this amplification of the conventional process of transcellular water and electrolyte movement by the presence of a very impermeant paracellular route and a pericryptal sheath, are unique requirements to generate the suction tension required for fecal dehydration.

This work was supported by projects BFI2003-05124 (Ministerio de Ciencia y Tecnología, Spain) and 2001SGR0142 (Generalitat de Catalunya, Spain) and the Wellcome Trust, UK. We are grateful to Dr. Carme Villà for plasma ion determinations and the support of the Confocal Service and the ICP-OES Service, Serveis Científicotècnics, Universitat de Barcelona. E.C. was recipient of a grant from MEC (Spain).

References

Abramoff, M.D., Magelhaes, P.J., Ram, S.J. 2004. Image Processing with ImageJ. *Biophotonics Int*. **11:**36–42

Asher, C., Wald, H., Rossier, B.C., Garty, H. 1996. Aldosterone-induced increase in the abundance of Na^+ channel subunits. *Am. J. Physiol*. **271:**C605–C611

Barlet-Bas, C., Khadouri, C., Marsy Doucet, S. A. 1988. Sodium-independent in vitro induction of Na^+ K^+-ATPase by aldosterone in renal target cells: permissive effect of triiodothyronine. *Proc. Natl. Acad. Sci. USA* **85:**1707–1711

Campbell, D.J., Habener, J.F. 1986. Angiotensinogen gene is expressed and differentially regulated in multiple tissues of the rat. *J. Clin. Invest.* **78:**31–39

Campbell, S.E., Janicki, J.S., Weber, K.T. 1995. Temporal differences in fibroblast proliferation and phenotype expression in response to chronic administration of angiotensin II or aldosterone. *J. Mol. Cell. Cardiol.* **27:**1545–1560

Colegio, O.R., Van Itallie, C., Rahner, C., Anderson, J.M. 2003. Claudin extracellular domains determine paracellular charge selectivity and resistance but not tight junction fibril architecture. *Am. J. Physiol.* **284:**C1346–C1354

Cristià E., Afzal I., Pérez-Bosque A., Amat C., Moretó M., Naftalin R.J. 2005. Pericryptal colon fibrosis induced by low sodium diets is mediated by aldosterone. *J. Membrane Biol.* **206:**53–59

De los Rios, A.D., Labajos, M., Manteca, A., Morell, M., Souviron, A. 1980. Stimulatory action of angiotensin II on water and electrolyte transport by the proximal colon of the rat. *J. Endocrinol.* **86:**35–43

Dolman, D., Edmonds, C.J., Salas-Coll, C. 1978. Effect of aldosterone on lithium permeability of rat colon mucosa. *Experientia* **34:**1174–1175

Duc, C., Farman, N., Canessa, C., Bonvalet, J., Rossier, B.C. 1994. Cell-specific expression of epithelial sodium channel α,β, and γ subunits in aldosterone-responsive epithelia from the rat: localization by in situ hybridization and immunocytochemistry. *J. Cell Biol.* **127:**1907–1921

Fardella, C.E., Mosso, L. 2002. Primary aldosteronism. *Clin. Lab.* **48:**181–190

Fromm, M., Hegel, U. 1978. Segmental heterogeneity of epithelial transport in rat large intestine. *Pfluegers Arch.* **378:**71–78

Fukushima, K., Naito, H., Funayama, Y., Yonezawa, H., Haneda, S., Shibata, C., Sasaki, I. 2004. In vivo induction of prostasin mRNA in colonic epithelial cells by dietary sodium depletion and aldosterone infusion in rats. *J. Gastroenterol.* **39:**940–947

Funder, J.W., Pearce, P.T., Smith, R., Smith, A.I. 1988. Mineralcorticoid action: target tissue specificity is enzyme, not receptor, mediated. *Science* **242:**583–585

Garty, H., Benos, D.J. 1988. Characteristics and regulatory mechanisms of the amiloride-blockable Na^+ channel. *Physiol. Rev.* **68:**309–373

Hirasawa, K., Sato, Y., Hosoda, Y., Yamamoto, T., Hanai, H. 2002. Immunohistochemical localization of angiotensin II receptor and local renin-angiotensin system in human colonic mucosa. *J. Histochem. Cytochem.* **50:**275–282

Horster, M., Fabritius, J., Buttner, M., Maul, R., Weekwerth, P. 1994. Colonic-crypt-derived epithelia express induced ion transport differentiation in monolayer cultures on permeable matrix substrata. *Pfluegers Arch* **426:**110–120

Jayaraman, S., Song, Y., Vetrivel, L., Shankar, L., Verkman, A.S. 2001. Non-invasive fluorescence measurement of salt concentration in the airway surface liquid. *J. Clin. Invest.* **107:**317–324

Klahr, S., Morrissey, J.J. 1997. Comparative study of ACE inhibitors and angiotensin II receptor antagonists in interstitial scarring. *Kidney Int. Suppl.* **63:**S111–S114

Molteni, A., Moulder, J.E., Cohen, E.F. 2000. Control of radiation-induced pneumopathy and lung fibrosis by angiotensin-converting enzyme inhibitors and an angiotensin II type 1 receptor blocker. *Int. J. Radial Biol.* **76:**523–532

Naftalin, R.J. 2004. Alterations in colonic barrier function caused by a low sodium diet or ionizing radiation. *J. Envir. Path. Toxicol. Oncol.* **23:**79–97

Naftalin, R.J. Pedley, K.C. 1999. Regional crypt function in rat large intestine in relation to fluid absorption and growth of the pericryptal sheath. *J. Physiol.* **514:**211–227

Naftalin, R.J., Zammit, P.S., Pedley, K.C. 1999. Regional differences in rat large intestinal crypt function in relation to dehydrating capacity in vivo. *J. Physiol.* **514:**201–210

Narikiyo, T., Kitamura, K., Adachi, M., Miyoshi, T., Iwashita, K., Shiraishi, N., Nonoguchi, H., Chen, L., Chai, K.X., Chao, J., Tomita, K. 2002. Regulation of prostasin by aldosterone in the kidney. *J. Clin. Invest.* **109:**401–408

Paul, M., Wagner, J., Dzau, V.J. 1993. Gene expression of the renin-angiotensin system in human tissue. Quantitative analysis by the polymerase chain reaction. *J. Clin. Invest.* **91:**2058–2064

Peart, W.S. 1969. The renin-angiotensin system: a history and review of the renin-angiotensin system. *Proc. R. Soc. Lond. B.* **173:**317–325

Rasband, W.S. 1997–2005. Image J. U. S. National Institutes of Health, Bethesda, Maryland, USA, http://rsb.info.nih.gov/ij/

Schulzke, J.D., Fromm, M., Hegel, U. 1986. Epithelial and subepithelial resistance of rat large intestine: segmental differences, effect of stripping, time course, and action of aldosterone. *Pfluegers Arch.* **407:**632–637

Shlyonsky, V., Goolaerts, A., Van Beneden, R., Sariban-Sohraby, S. 2005. Differentiation of epithelial Na^+ channel function. *J. Biol. Chem.* **280:**24181–24187

Stanton, B., Giebisch, G., Klein-Robbenhaar, G., DeFronzo, R., Giebisch Wade, G.J. 1985. Effects of adrenalectomy and chronic adrenal corticosteroid replacement on potassium transport in rat kidney. *J. Clin Invest.* **75:**1317–1326

Swaney, J.S., Roth, D.M., Olson, E.R., Naugle, J.E., Meszaros, J.G., Insel, P.A. 2005. Inhibition of cardiac myofibroblast formation and collagen synthesis by activation and overexpression of adenylyl cyclase. *Proc. Natl. Acad. Sci., USA* **102:**437–442

Thiagarajah, J.R., Griffiths, N.M., Pedley, K.C., Naftalin, R.J. 2002. Evidence for modulation of pericryptal sheath myofibroblasts in rat descending colon by transforming growth factor β and angiotensin II. *Gastroenterology.* **2:**4–15

Thiagarajah, J.R., Jayaraman, S., Naftalin, R.J., Verkman, A.S. 2001a. In vivo fluorescence measurement of Na^+ concentration in the pericryptal space of mouse descending colon. *Am. J. Physiol.* **281:**C1898–C1903

Thiagarajah, J.R., Pedley, K.C., Naftalin, R.J. 2001b. Evidence of amiloride-sensitive fluid absorption in rat descending colonic crypts from fluorescence recovery of FITC-labeled dextran after photobleaching. *J. Physiol.* **536:**541–553

Tsuruda, T., Kato, J., Cao, Y.N., Hatakeyama, K., Masuyama, H., Imamura, T., Kitamura, K., Asada, Y., Eto, T. 2004. Adrenomedullin induces matrix metalloproteinase-2 activity in rat aortic adventitial fibroblasts. *Biochem. Biophys. Res. Commun.* **325:**80–84

Tsuruda, T., Kato, J., Hatakeyama, K., Masuyama, H., Cao, Y.N., Imamura, T., Kitamura, K., Asada, Y., Eto, T. 2005. Antifibrotic effect of adrenomedullin on coronary adventitia in angiotensin II-induced hypertensive rats. *Cardiovasc. Res.* **65:**921–929

Weber, K.T. 1997. Fibrosis, a common pathway to organ failure: angiotensin II and tissue repair. *Semin. Nephrol.* **17:**467–491